Liquid Crystals
Publication details, including instructions for authors and subscription information:
http://www.informaworld.com/smpp/title~content=t713926090

Possible structures for the lamellar-isotropic (Lam-I) and lamellar-nematic (Lam-N) liquid crystalline phases

Neha M. Patel[a]; Ishtiaque M. Syed[a]; Charles Rosenblatt[a]; Marko Prehm[b]; Carsten Tschierske[b]
[a] Department of Physics, Case Western Reserve University, Cleveland, Ohio 44106-7079, USA [b] Martin-Luther-Universität Halle-Wittenberg, Institute of Organic Chemistry, 06120 Halle, Germany

To cite this Article Patel, Neha M. , Syed, Ishtiaque M. , Rosenblatt, Charles , Prehm, Marko and Tschierske, Carsten(2005) 'Possible structures for the lamellar-isotropic (Lam-I) and lamellar-nematic (Lam-N) liquid crystalline phases', Liquid Crystals, 32: 1, 55 — 61
To link to this Article: DOI: 10.1080/02678290512331324011
URL: http://dx.doi.org/10.1080/02678290512331324011

Liquid Crystals, Vol. 32, No. 1, January 2005, 55–61

Possible structures for the lamellar–isotropic (Lam-I) and lamellar–nematic (Lam-N) liquid crystalline phases

NEHA M. PATEL†, ISHTIAQUE M. SYED†, CHARLES ROSENBLATT*†, MARKO PREHM‡ and CARSTEN TSCHIERSKE‡

†Department of Physics, Case Western Reserve University, Cleveland, Ohio 44106-7079, USA
‡Martin-Luther-Universität Halle-Wittenberg, Institute of Organic Chemistry, 06120 Halle, Germany

(*Received 26 July 2004; accepted 30 August 2004*)

The three refractive indices of a liquid crystal that exhibits lamellar analogues of the three-dimensional isotropic, nematic, and smectic A phases are reported as functions of temperature for the Lam-I and Lam-N phases. The data suggest a number of striking behaviour types. The orientational distribution of the mesogenic moieties becomes more highly peaked in two dimensions on cooling from the Lam-I to the Lam-N phase; the two-dimensional order associated with mesogenic director **n** in the Lam-N phase is weak; and conformational changes in the side chain result in an increase in the refractive index perpendicular to the lamellae with decreasing temperature in the Lam-N phase.

1. Introduction

In recent years there has been increasing interest in the self-organization of simple organic components into more complex structures [1, 2]. Tschierske *et al*. have demonstrated that structures having the mesogenic moiety shown in figure 1, and with long semiperfluorinated lateral alkyl chains R [e.g. R=$OCH_2C^*H(CH_3)O(CH_2)_{11}C_8F_{17}$] can exhibit novel lamellar liquid crystalline phases, viz. lamellar isotropic (Lam-I), lamellar-nematic (Lam-N), and lamellar smectic A (Lam-A) phases [2–7], which are described below. Compound **1** (figure 1), which we refer to as 'mpp88,' exhibits all three of these lamellar phases (many materials exhibit only some of these phases) and moreover is designed to have low transition temperatures and a broad Lam-N region. Its phase sequence on heating corresponds to crystal–112°C–Lam-A–125°C–Lam-N–139°C–Lam-I–169°C–3D isotropic. The Lam-A phase can be supercooled to 77°C, below which an unidentified phase arises until crystallization occurs around 47°C. Synthesis details will be reported elsewhere [8]. A schematic representation of the three phases, at least in terms of our understanding prior to this work, is shown in figure 2. The segregation into mesogenic lamellar and partially perfluorinated alkyl subregions is due to the molecules' three incompatible moieties: a rigid aromatic core, two polar diol groups that interact with other diol groups via cooperative hydrogen bonding, and the partially perfluorinated pendant chain R. The perfluorinated chain has the effect of separating the mesogenic sublayers, in this case with a periodicity b=4.4 nm [7], which appears to be approximately independent of temperature through all three phases of this material.

In the Lam-N phase, figure 2(*b*), the orientational distribution function of the mesogenic groups lies primarily in the lamellar (xy) plane and is peaked along the x-axis. In the Lam-A phase, figure 2(*c*) a periodic structure sets in within the mesogenic sublayer. Until now our picture of the Lam-I phase, figure 2(*a*) consisted of hydrogen-bonded, orientationally-correlated mesogenic groups having a correlation length somewhat smaller than optical wavelengths, with the correlated groups randomly oriented in the xy-plane. The results presented herein, however, will suggest that the orientational distribution of the mesogenic groups in the Lam-I phase is highly disordered along the z-axis as well as within the xy-plane. In all three phases the thickness of the mesogenic sublayer is of order 1 nm [2], indicating that the mesogenic sublayer can be several molecular widths thick. Finally, although the pendant chain R is chiral for mpp88, effects of chirality on the phase sequence, elastic, and optical properties seem minimal.

In previous work we examined the twist elastic constant K_{22} and associated viscosity γ_1 in the Lam-N phase [9], finding values for K_{22} more than an order of magnitude smaller than values typical of ordinary three-dimensional nematic phases. Recently we have begun

*Corresponding author. Email: rosenblatt@case.edu

Liquid Crystals ISSN 0267-8292 print/ISSN 1366-5855 online © 2005 Taylor & Francis Ltd
http://www.tandf.co.uk/journals
DOI: 10.1080/02678290512331324011

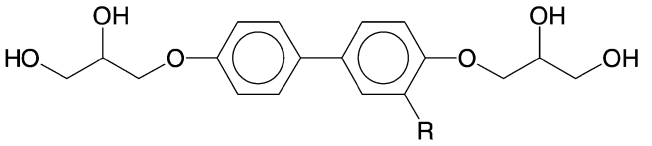

Compound **1**: R = $OCH_2C^*H(CH_3)O(CH_2)_{11}C_8F_{17}$

Compound **2**: R = $(CH_2)_3C_{10}F_{21}$

Figure 1. Structures of compound **1**, known as mpp88, and compound **2**, known as 3/10.

to examine collective fluctuations of the mesogenic director, both within and outside of the mesogenic sublayers. In order to analyse our light scattering data, we have measured the three refractive indices of mpp88 in the Lam-I and Lam-N phases as functions of temperature. In this paper we report on the measured refractive indices, which provide significant insight into the architecture and ordering of the molecules in the Lam-I and Lam-N phases.

2. Experimental methods and results

The Lam-N phase is biaxial [10], with refractive index n_s parallel to the mesogenic director **n**, which we define as the average orientation of the mesogenic moieties in the sublayer; see figure 2 (*b*). Index n_o is perpendicular to **n** and parallel to the lamellar planes; and index n_p is perpendicular to the plane of the lamellae. Ordinarily, one would align the liquid crystal first with the lamellae parallel to the substrates of the cell and measure n_s and n_o by interference methods, or determine the birefringence $\Delta n_{so} \equiv n_s - n_o$ for an optical polarization parallel to the lamellar planes by standard retardation methods. One then would align the liquid crystal with the lamellae perpendicular to the cell walls, with **n** lying vertically or horizontally. By judicious choice of alignment orientations, in principle one could extract all three refractive indices.

Although all alignments are possible over very small regions, achieving an alignment of the lamellae perpendicular to the substrates is particularly difficult. Neither magnetic nor electric fields, nor a variety of surface treatment techniques, would yield a large monodomain in which the lamellae lie perpendicular to the substrates. We found that shearing of the cell gives the best results, inducing a very good—but not quite perfect—monodomain structure over small regions of order several hundred μm, with the lamellae parallel to the cell walls and **n** parallel to the shear direction (in the Lam-N phase). As a result, we approached the problem in three steps. First, Δn_{so} was obtained as a function of temperature by standard birefringence techniques, where the size of the sample probed by the laser was kept small, to ~50 μm. We remark that attempts to obtain n_s and n_o separately by interference techniques—this was attempted both by varying the wavelength of light and varying the angle of incidence at fixed wavelength [10]—were unsuccessful because of the not-quite-perfect alignment; Δn_{so} is much less sensitive to these imperfections. Next, the cell was

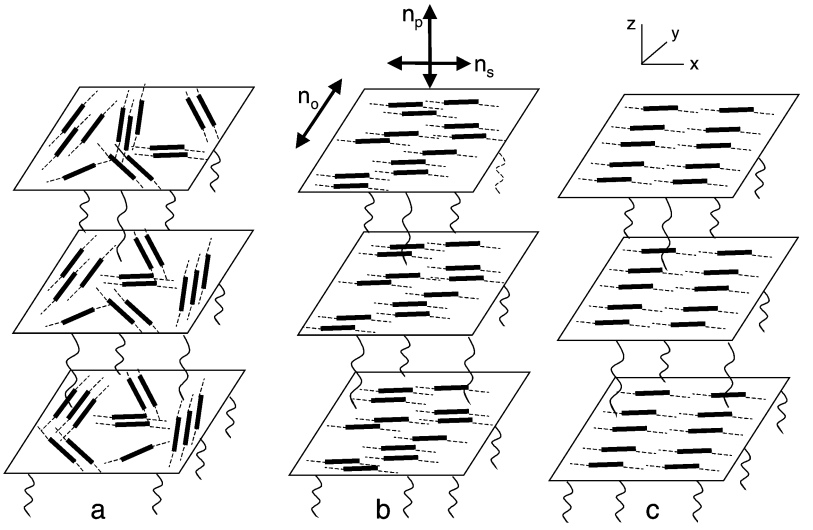

Figure 2. Schematic representation of lamellar phases. (*a*) Lam-I phase (according to the view-point prior to this work the molecules are aligned on average parallel to the layer planes, but without long range orientational correlations within the layer planes; based on the work presented here, the Lam-I phase is now believed to have a large component of the mesogenic director oriented out of the sublayer plane; see also figure 8). (*b*) Lam-N phase; and (*c*) Lam-A phase. Definitions of the three refractive indices are shown by heavy double arrows. Coordinate system *xyz* for the sample frame of reference is shown at the top of the figure.

rotated by an angle β about the shear axis (x-axis) and the optical retardation, which for $\beta \neq 0$ is a function of all three refractive indices and the rotation angle β, was measured as a function of temperature. Finally, the refractive index n_{iso} in the 3D isotropic phase was obtained by an interference technique; values of $n_{iso}(T)$ in other phases were obtained by using the Clausius–Mossotti relationship in conjunction with measurements of the relative density of the liquid crystal vs. temperature. The three refractive indices n_s, n_o, and n_p were then calculated as a function of temperature from these three measurements. In addition to alignment benefits, this approach has the additional advantage of using the same cell for two of the three measurements.

The first two measurements were performed using a retardation method. Two glass microscope slides were cut and cleaned sequentially in detergent, water, acetone, and ethanol. One slide of dimension $20 \times 10\,mm^2$ was cemented to the base of an Instec hot stage, and the other slide of dimension $20 \times 2\,mm^2$ was attached to a micrometer-controlled movable tongue and placed over the first slide. The short axis of the movable slide was oriented along the direction of motion. Two mylar strips of nominal thickness 12.5 μm served as spacers between the glass slides, and a clamp was affixed so that the spacing between the slides would be maintained, even during shearing. In order to determine the thickness of the cell, the empty cell was heated to 150°C, corresponding to the Lam-I phase, and placed on a stepping motor-controlled rotation stage. Light from a He-Ne laser passed through the cell, and the periodic transmitted intensity was measured as a function of rotation angle. Based on this interferometric measurement [10], a cell thickness $d = 19.7 \pm 0.1\,\mu m$ was deduced. From an observation of interference fringes under an incoherent green light, we observed on translation of the top slide that the thickness of the cell changed by less than $\Delta d = 0.1\,\mu m$. The cell was filled in the 3D isotropic phase with mpp88, cooled into the Lam-N phase, and then sheared. The hot stage was placed into a retardation apparatus (figure 3) in which light from a He-Ne laser, and polarized at 45° with respect to the shear (x) axis, passed through a Pockels cell modulated at $f = 530\,Hz$, the sample, a lens of focal length 51 mm located a distance slightly larger than its focal length behind the sample, and an analyser. A 500 μm diameter pinhole and detector were placed downstream, such that a real image of the sample enlarged by a factor of 12.5 impinged on the detector. This facilitated *in situ* visual inspection, and allowed us to select only those regions (<50 μm) of the sample that were reasonably well-aligned. The output from the detector was fed into a lock-in amplifier referenced at frequency f, whose output in turn was integrated and used as a programming voltage for a d.c. voltage supply that was fed back into the Pockels cell to nullify the d.c. output from the detector. In this way the d.c. Pockels cell voltage V was automatically adjusted to compensate—and thus facilitate a measurement of—the temperature-dependent sample retardation $\alpha_{so}(T)$ [11], where

$$\alpha_{so}(T) = kd\Delta n_{so}(T) = kd[n_s(T) - n_o(T)]. \qquad (1)$$

Here $k = 2\pi/\lambda = 9.93 \times 10^4\,cm^{-1}$ for $\lambda = 632.8\,nm$ He-Ne light. Figure 4 shows $\Delta n_{so}(T) = n_s(T) - n_o(T)$ in the Lam-I and Lam-N phases as the sample was cooled at a rate of $400\,mK\,min^{-1}$. On sampling other regions of the cell, we found qualitatively similar curves, although the magnitude of Δn_{so} vs. T varied by up to ±15% from run to run.

On rotating the cell by an angle β about the shear (and therefore the x-axis), the incoming polarization breaks into a component parallel to **n** along the x-axis with refractive index n_s and a second component in the yz-plane that depends on both n_o and n_p. For the component along **n**, the temperature-dependent angle γ_s

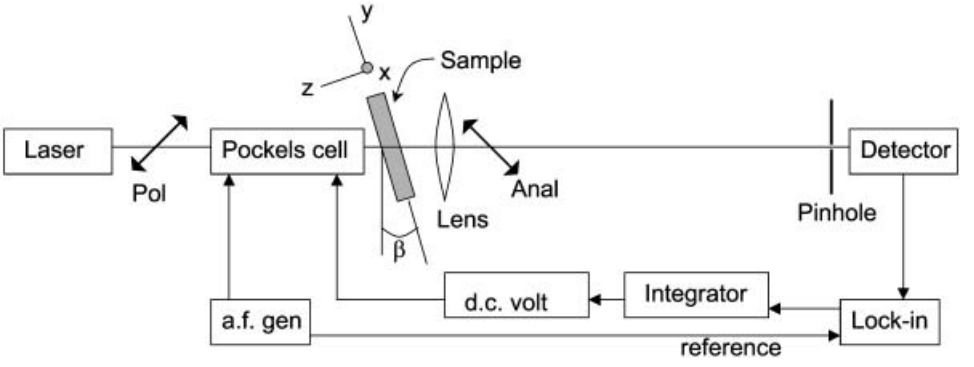

Figure 3. Schematic view of experiment. Pol corresponds to polarizer, Anal to analyser. Angle $\beta = 0°$ for measurements of Δn_{so} and $\beta = 18°$ for measurements of α_{sop}.

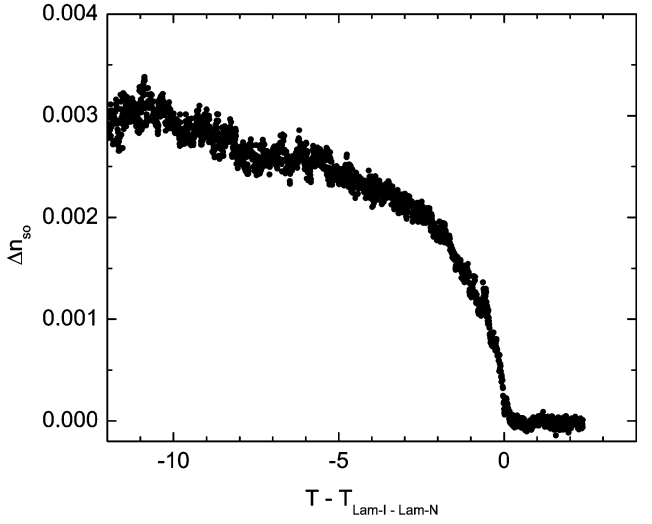

Figure 4. Measured birefringence $\Delta n_{so}(T)$ vs. temperature. See text for discussion of data reproducibility.

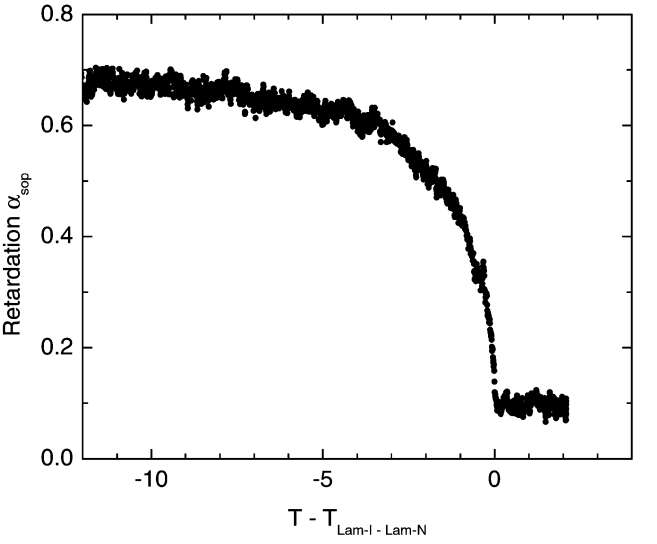

Figure 5. Retardation α_{sop} vs. temperature for cell rotated by angle $\beta=18^\circ$ about the shear axis.

inside the liquid crystal is determined from Snell's law, viz. $\gamma_s(T)=\sin^{-1}[(\sin\beta)/n_s]$. For the other component, the effective temperature-dependent refractive index $n_{op}(T,\gamma_{op})=n_o n_p\left(n_o^2\sin^2\gamma_{op}+n_p^2\cos^2\gamma_{op}\right)^{-1/2}$, where $\gamma_{op}(T)$ is the temperature-dependent angle inside the liquid crystal and determined implicitly from $\gamma_{op}(T)=\sin^{-1}[(\sin\beta)/n_{op}]$. The relative retardation $\alpha_{sop}(T)$ of the two components is given by [10]

$$\alpha_{sop}(T)= kd\left[\frac{n_s}{\cos\gamma_s}+\sin\beta(\tan\gamma_{op}-\tan\gamma_s)-\frac{n_{op}}{\cos\gamma_{op}}\right] \quad (2)$$

where n_s, n_o, n_p, γ_s, and γ_{op} all depend on temperature. Using the modulated Pockels cell, α_{sop} was measured as a function of angle β at a fixed temperature $T=142^\circ$C in the Lam-I phase; for $\beta=18^\circ$ (this is an angle sufficiently large that n_p contributes significantly to α_{sop}) we found $\alpha_{sop}(T=142^\circ)=0.10^{+0.04}_{-0.03}$ rad. (Note that the enlarged real image at the detector allowed us to measure α_{sop} at precisely the same position in the sample for both $\beta=0^\circ$ and $\beta=18^\circ$). The moderately large relative error bars are attributed to the rather small retardation in the Lam-I phase and to the not-quite-perfect monodomain texture of the liquid crystal. The cell, fixed in orientation at $\beta=18^\circ$, was then cooled into the nematic phase and the change in α_{sop} was measured as a function of temperature. Figure 5 shows $\alpha_{sop}(T)$ at $\beta=18^\circ$.

The third measurement involves the average refractive index. Such a measurement is not possible in any of the lamellar phases—including the Lam-I phase—due to scattering from the random domain structures. Instead, the measurement must be performed in the 3D isotropic phase, at approximately $T=170^\circ$C. A rigid optical cavity was constructed of high refractive index glass ($n=1.91$) separated by aluminum foil spacers of thickness 6 μm, and then cemented with high temperature epoxy. High index glass was used in order to facilitate a large reflectivity coefficient at the liquid crystal—glass interfaces. The cell was mounted in the hot stage, and the thickness measured at 170°C by an interferometric technique in which the cell is rotated and the intensity measured as a function of rotation angle [10]; the spacing was determined to be $d=7.2\pm0.2$ μm. The cell was then filled with mpp88 in the 3D isotropic phase and transferred into a Cary 500 Scan UV-Vis-NIR spectrophotometer. Spectra were taken of the optical transmission through the cell in the wavelength range $610\leqslant\lambda\leqslant640$ nm, and the refractive index n_{iso} was determined from $n_{iso}=\lambda_{m+1}\lambda_m/2d(\lambda_{m+1}-\lambda_m)$, where m is the order of the transmission maximum. An isotropic refractive index $n_{iso}=1.52\pm0.02$ at $T=170^\circ$C was obtained.

In order to determine $n_{iso}(T)$ vs. temperature, the relative density of the liquid crystal was measured as a function of T by partially filling a precision capillary of thickness 100 μm with mpp88. The area of the filled region was measured as a function of temperature, and the relative density ρ_r was extracted from the ratio of the filled area at $T=170^\circ$C (1°C above the transition to the Lam-I phase) to its area at temperature T. Thus, by definition $\rho_r=1$ at $T=170^\circ$C. Data are shown in figure 6, and are consistent with thermal expansion coefficients of numerous other organic materials.

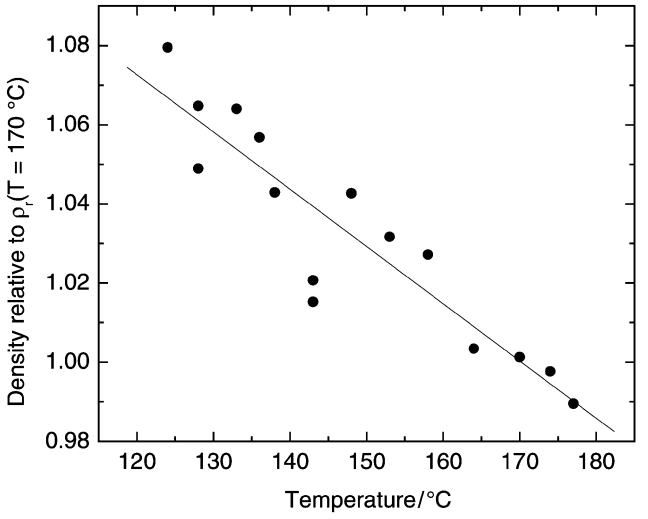

Figure 6. Mass density of mpp88 relative to the density at T=170°C in the 3D isotropic phase. Solid line represents linear fit to the data.

Because of the large area (and the associated large temperature difference of ~1°C across this area) needed for the measurement, it was not possible to observe density jumps at the various phase transitions. Instead, the data ρ_r vs. T were fitted to a straight line over this region. We then used the Clausius–Mossotti relationship $\left(n_{iso}^2-1\right)/\left(n_{iso}^2+2\right)=a\rho_r$, where the constant a is proportional to the average molecular polarizability and to the number density at the temperature at which ρ_r=1, to obtain n_{iso} vs. temperature. Since $n_{iso}=1.52\pm 0.02$ at T=170°C, where we have defined ρ_r=1, we find that a=0.3040. Using the linear fit for ρ_r vs. T in figure 6, we employ Clausius–Mossotti to obtain $n_{iso}(T)$; results are shown in figure 7. The three refractive indices n_s, n_o, and n_p as functions of temperature were then deduced from the data using equations (1) and (2), γ_s, γ_{op} and $n_{iso}^2=\left(n_s^2+n_o^2+n_p^2\right)/3$; the results are shown in figure 8, where the error bar corresponds to run-to-run variations mostly in α_{sop} at β=18° (and to a smaller extent in Δn_{so}), but not in the determination of n_{iso} or systematic errors due to uncertainty in thickness measurements. Thus the error reflects an overall shift of the n_p curve relative to n_s and n_o, rather than an error in n_s-n_o or point-to-point uncertainties in n_s, n_o and n_p.

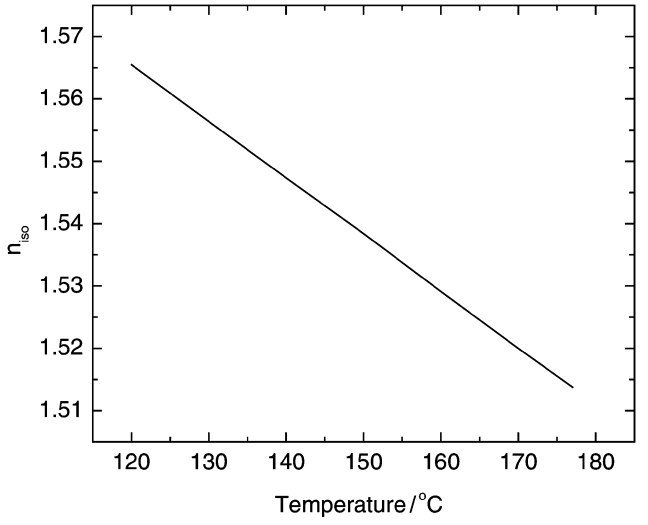

Figure 7. n_{iso} vs. temperature calculated using the Clausius–Mossotti relationship and a linear fit to the relative density data in figure 6.

3. Discussion

Let us first consider the refractive indices in the Lam-I phase. That the retardation α_{sop} in this phase at β=18° is relatively small, and that both n_s and n_o increase on cooling into the Lam-N phase, indicate that our previous picture for the Lam-I phase, cf. figure 2 (*a*), may be incomplete or incorrect in certain details. For example, consider a scenario in which the mesogens lie approximately in the xy-plane in the Lam-I phase. One could imagine a conformational change around the bond between the two phenyl rings occuring at the phase transition. If the two rings were strongly twisted around this bond, e.g. if the dihedral angle were close to 90° in the Lam-I phase, then the π-systems of the two rings would be nearly independent. However, if the

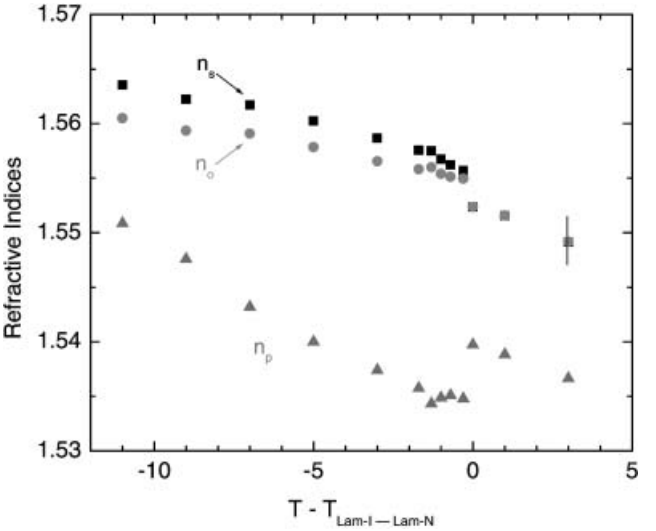

Figure 8. Derived refractive indices n_s (■), n_o (●), and n_p (▲) at several temperatures above and below the phase transition. The error bars, which apply to n_s-n_p (or equivalently n_o-n_p), reflect the reproducibility of results for α_{sop} at β=18° and for Δn_{so}, but not in the determination of n_{iso} or systematic errors due to uncertainty in thickness measurements. See text for a discussion of the uncertainty in n_s-n_o.

rings were to become co-planar in the Lam-N and Lam-A phases, the conjugation of the π-systems would give a component of refractive index in the lamellar plane that is larger in the lower temperature lamellar phases than in the Lam-I phase. This would be accompanied, of course, by an associated change in n_{iso}, which would mean that all the refractive indices would need to be shifted in the Lam-N and Lam-A phases. Such a mechanism would not induce a significant change in the periodic spacing b with temperature, consistent with X-ray results [6]. Nevertheless, the moderate decrease in n_p at the transition is difficult to reconcile with this mechanism, as such a conformational change would be expected to have little effect on n_p.

We shall proceed with the conjecture that the mesogenic groups in the Lam-I phase are disordered in three dimensions on length scales short compared with a wavelength of light, although cooperative hydrogen bonding facilitates short range order on molecular length scales. In this picture the mesogenic sublayer would appear optically isotropic, with a refractive index $n_{mesogenic}$. Similarly, a three-dimensionally disordered side chain sublayer would be optically isotropic, with index $n_{sidechain}$. This scenario would correspond to a Lam-I phase in which each of the two sublayers is disordered, i.e. to nanophase separation into sublayers with no inherent orientational order within the sublayers. In this case a 'form birefringence' still would exist [10]. To estimate the form birefringence, we take the side chain sublayer to be approximately three times thicker than the mesogenic sublayer and we assume reasonable values $n_{mesogenic} \approx 1.63$ and $n_{sidechain} \approx 1.48$. Such values would be consistent with the relative volume of each of the two sublayers and with the data in figure 8. Due to the layered structure of the Lam-I phase, one therefore would expect a form birefringence $n_s - n_p = n_o - n_p$ of approximately 0.01, which is similar to the observed value of $n_s - n_p$ in the Lam-I phase as seen in figure 8. To be sure, the data are not sufficiently accurate to conclude whether the individual mesogenic sublayers are completely isotropic or whether the mesogens are oriented preferentially—but not completely—within the sublayer.

On cooling into the Lam-N phase we observe that the three refractive indices change rapidly with temperature. *The way in which these quantities vary with temperature is key to our picture of the transition*. For the rapid—and apparently nearly equal—increases to occur in *both* n_s and n_o just below the transition temperature, it is necessary that the orientational distribution of the mesogenic unit changes rapidly with temperature from complete—or nearly complete—three-dimensional disorder in the Lam-I phase (see figure 9) to being somewhat more peaked within the mesogenic sublayer in the Lam-N phase; the same argument would result in a rapid decrease of n_p with temperature. Let us consider a thought experiment. If the mesogens were disordered in only two—rather than in three—dimensions in the Lam-I phase, as in figure 2 (*a*), then n_o would decrease with decreasing temperature and n_p would be nearly temperature-independent on cooling into the Lam-N phase. But this behaviour is not observed. Rather, the initial increase in both n_s and n_o and the decrease in n_p indicate that the orientational distribution of the mesogenic axes becomes more sharply peaked in the xy-plane on cooling into the Lam-N phase. Just below the transition temperature Δn_{so} is small compared with the increases in n_s and n_o, indicating that the orientational distribution is nearly oblate uniaxial, and the transition into the Lam-N phase is apprarently continuous (cf. figure 4). With decreasing temperature the mesogenic director profile becomes more peaked along the shearing direction, and the system becomes more strongly biaxial with $n_s \neq n_o \neq n_p$. Owing to the relative smallness of Δn_{so} it may be that our previous estimate for the dielectric anisotropy $\Delta\varepsilon$ was too large [9]. Had we used a smaller $\Delta\varepsilon$ we would have calculated yet a smaller twist elastic constant K_{22} for the Lam-N phase, indicating an even greater difference from typical 3D nematic behaviour.

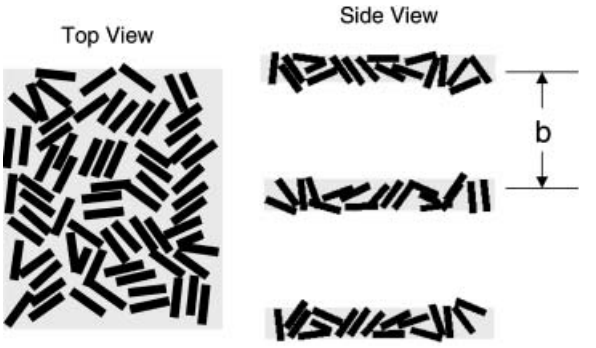

Figure 9. Schematic view of Lam-I phase in which there is considerable out-of-sublayer orientational disorder of the mesogenic director. Left: top view upon the sublayers. Right: side view parallel to the sublayers.

Briefly turning to uncertainties in our measured data, we first note that the apparent continuous nature of the Lam-I–Lam-N transition is unaffected by the uncertainty in Δn_{so} that arises because of not-quite-perfect alignment. As noted above, the Δn_{so} vs. T traces measured at different points in the cell are nearly identical, varying only in magnitude by $< \pm 15\%$. As the temperature variation across the probed region of the sample is less than 25 mK, it is clear that the behaviour in figure 4 is *not* first order. Second, does the error bar

in figure 8, associated primarily with α_{sop} and thus with possible overall shifts of the n_p curve relative to n_s and n_o, affect our conclusion regarding the orientational distribution being more peaked in the xy-plane in the Lam-N phase? The answer is no: although the changes in refractive index reflect the *degree* of in-plane orientational order, there is no doubt that the trend indicates a jump in in-plane order on cooling into the Lam-N phase.

From figure 8 we also note that at approximately 2°C below the Lam-I–Lam-N transition the temperature derivatives of the refractive indices change, viz. n_s and n_o increase more slowly with decreasing temperature and n_p *increases* with decreasing temperature, where $|dn_p/dT|>|dn_{s,o}/dT|$. As one would expect the mesogenic director orientation to become more peaked in the xy-plane with decreasing temperature, this behaviour would require an increase in the order of the side chains. This would result in an increase of the refractive index n_p perpendicular to the lamellae and a decrease in the in-plane refractive indices, as observed. Interestingly, there is no observable change in the lamella-to-lamella spacing b, which indicates that despite the probable conformational changes in the side chains with temperature the density probably remains constant. The refractive index change can occur because of the existence of alkyl and perfluorinated alkyl segments in the side chain.

Amador and Pershan have shown [12] that thin (two-dimensional) free-standing films exhibit a small Nelson–Kosterlitz discontinuity [13] in polar tilt angle at the smectic A–smectic C phase transition. Moreover, de Gennes has discussed theoretically [14] the behaviour of two-dimensional nematics, and has shown that only 'quasi-nematic' order obtains. The orientational correlation $\langle[\varphi(\mathbf{r}_1)-\varphi(\mathbf{r}_2)]^2\rangle$ diverges for large $\mathbf{r}_1-\mathbf{r}_2$, where φ is the in-plane azimuthal orientation of the director **n**. The compound mpp88 clearly is not a two-dimensional system, as the mesogenic layers interact, if only weakly [9]. Nevertheless, the apparent continuous rise in Δn_{so} at the Lam-N transition is intriguing, and requires further investigation. It is also interesting that Δn_{so} remains moderately small, even at low temperatures, indicating a relatively small degree of in-plane nematic order. Although our experiment probed a seemingly well aligned region, and our system clearly is not two-dimensional, the apparent smallness of Δn_{so} could be due in part to large in-plane director fluctuations on short length scales. This is part of the motivation behind our related light scattering experiments.

Lamellar liquid crystalline phases bear many similarities with traditional three-dimensional phases. Yet, many of the properties are enigmatic, and will require considerable effort to unravel. Our refractive index measurements suggest that the previous picture of the two-dimensionally disordered mesogenic unit lying within the sublayer in the Lam-I phase may not be completely correct. Instead, we have conjectured that the mesogenic director **n** actually may have a significant component perpendicular to the lamellae. On entering the Lam-N phase, **n** lies mostly in the lamellar plane, but does not develop significant order in two dimensions as the temperature decreases. At this time these mechanisms remain speculation, and further work on these materials is clearly needed.

Acknowledgements

We thank Prof. Rolfe G. Petschek for useful discussions. This work was supported by the Deutsche Forschungsgemeinschaft under grants TS 39/11-3 and GRK 894, by the National Science Foundation under grant DMR-0345109, and by the Donors of the Petroleum Research Fund, administered by the American Chemical Society, under grant 37736-AC7.

References

[1] J.-M. Lehn. *Proc. nat. Acad. Sci.*, **99**, 4763 (2002).
[2] C. Tschierske. *J. mater. Chem.*, **11**, 2647 (2001).
[3] M. Prehm, X.H. Cheng, S. Diele, M.K. Das, C. Tschierske. *J. Am. chem. Soc.*, **124**, 12072 (2002).
[4] M. Kölbel, T. Beyersdorff, X.H. Cheng, C. Tschierske, J. Kain, S. Diele. *J. Am. chem. Soc.*, **123**, 6809 (2001).
[5] X.H. Cheng, M.K. Das, S. Diele, C. Tschierske. *Angew. Chem.*, **114**, 4203 (2002).
[6] X.H. Cheng, M. Prehm, M.K. Das, J. Kain, U. Baumeister, S. Diele, D. Leine, A. Blume, C. Tschierske. *J. Am. chem. Soc.*, **125**, 10977 (2003).
[7] M. Prehm, S. Diele, M.K. Das, C. Tschierske. *J. Am. chem. Soc.*, **125**, 614 (2003).
[8] M. Prehm, C. Tschierske (to be published).
[9] N.M. Patel, M.R. Dodge, M.H. Zhu, R.G. Petschek, C. Rosenblatt, M. Prehm, C. Tschierske. *Phys. Rev. Lett.*, **92**, 015501 (2004).
[10] M. Born, E. Wolf. *Principles of Optics*. Pergamon, Oxford (1980).
[11] C. Rosenblatt, F.F. Torres de Araujo, R.B. Frankel. *Biophys. J.*, **40**, 83 (1982).
[12] S.M. Amador, P.S. Pershan. *Phys. Rev. A*, **41**, 4326 (1990).
[13] D.R. Nelson, J.M. Kosterlitz. *Phys. Rev. Lett.*, **39**, 1201 (1977).
[14] P.G. DeGennes. *Symp. Faraday Soc.*, **5**, 16 (1971).